

# Rose-Hulman Undergraduate Mathematics Journal

---

Volume 10  
Issue 2

Article 1

---

## Using Biomechanical Optimization to Interpret Dancers' Pose Selection for a Partnered Spin

Megan E. Selbach-Allen  
U.S. Naval Academy, [selbachallenm@yahoo.com](mailto:selbachallenm@yahoo.com)

Follow this and additional works at: <https://scholar.rose-hulman.edu/rhumj>

---

### Recommended Citation

Selbach-Allen, Megan E. (2009) "Using Biomechanical Optimization to Interpret Dancers' Pose Selection for a Partnered Spin," *Rose-Hulman Undergraduate Mathematics Journal*: Vol. 10 : Iss. 2 , Article 1.  
Available at: <https://scholar.rose-hulman.edu/rhumj/vol10/iss2/1>

# Using Biomechanical Optimization to Interpret Dancers' Pose Selection for a Partnered Spin

Megan E. Selbach-Allen

October 12, 2009

## Introduction

Many people all over the world enjoy swing dancing. Dancers often talk about using the laws of physics in performing their physically rigorous jumps, lifts, and spins. However, they do not have mathematical evidence to support these claims. Our goal was to determine whether expert swing dancers physically optimize their pose for a partnered spin. In a partnered spin, two dancers connect hands and spin around a single vertical axis. We describe the pose of a couple by the angles of their joints in a two-dimensional plane. Optimal values for these angles were outputs of an optimization model that gave the ideal pose for a couple. A biomechanical model built in Mathematica allowed comparisons to live dancers with the use of a motion capture system.

The optimization objective is to maximize estimated angular acceleration. The model considers only external forces and neglects internal forces. It consists of equations derived from physical principles such as Newton's laws and moment of inertia calculations that govern how people move. Using numerical non-linear optimization we found the pose for each couple that maximizes their angular acceleration. Different dancers are differently sized, so every couple has a different optimal pose. Each couple's optimal pose was compared to the pose they actually assumed for the spin.

Our motion capture system recorded the three-dimensional location of each of the marked body joints. We used this data to determine the angles of the joints to calculate the couple's actual pose, and predict their angular acceleration in the

spin. This predicted acceleration was then compared to the optimal acceleration to determine a fraction of optimal for each couple. We hypothesized that expert swing dancers would achieve a higher fraction of their optimal acceleration than beginners. We were unable to determine a statistically significant difference between the poses of expert and beginner dancers. However, the optimal pose predicted by the model was intuitively reasonable.

## 1 Why swing dance and physics?

Lindy Hop is an athletic style of dancing that originated in the 1920s and is now danced recreationally and competitively. It is an American folk partner dance form that originated in the Harlem of the 1920's and 1930's. Today Lindy Hop is danced to very fast music and can involve aerial tricks in addition to fancy footwork. Advanced dancers often train intensely for five to ten years before reaching the top levels of competition. While work has been done to examine how Ballet dancers make use of physics in performing [1] [2] , no one has studied swing dancers.

A rhythm circle is a movement in which a couple spins as a unit around a single vertical axis. A good rhythm circle would look smooth, but also involve the dancers rotating fast. When discussing this movement, dancers often talk about minimizing moment of inertia or the need to create torque to spin. To our knowledge we are the first to study this movement and determine quantitatively if their descriptions are accurate.

We developed a few candidate mathematical objectives for describing the best pose. We considered moment of inertia, angular acceleration, and angular velocity as possible objectives that better dancers might minimize or maximize. Angular acceleration was ultimately chosen as the objective value because it was easier to calculate than angular velocity, and since angular acceleration is what allows the couples to reach their max speeds it still has a correlation to maximizing speed. Additionally, this value takes into account the need to produce force from the feet, torque, along with the need to minimize moment of inertia. The actual value of the objective will vary for each couple because it will be determined by their individual sizes.

We created a model to estimate the torques the dancers create to propel themselves in a circle, along with their moments of inertia. Rather than directly calculate torque, we used a surrogate method to estimate the external forces acting on the dancer.

We used a numerical optimization scheme in Mathematica to find a pose that maximized angular acceleration for each couple. The problem is nonlinear because of

Lengths	
$mLf$	Length of forearms of leader
$mLb$	Length of biceps of leader
$mLt$	Length of torso of leader
$mLq$	Length of upper leg (quads) of leader
$mLc$	Length of lower leg (calf) of leader
$fLf$	Length of forearms of follower
$fLb$	Length of biceps of follower
$fLt$	Length of torso of follower
$fLq$	Length of upper leg (quads) of follower
$fLc$	Length of lower leg (calf) of follower

Table 1: Table of the notation we used to describe the dancers bodies.

the presence of trigonometric functions relating the joint angles, which determine the pose, to the objective function. Mathematica’s “NMaximize” function implements a global non-linear optimization scheme. The optimization problem was particularly challenging because it was non-linear and high dimensional. Our decision variables were the 14 angles that defined the couple’s pose. The objective was to maximize estimated rotational acceleration.

## 2 The Model

### 2.1 Defining Body Segment Lengths

Table 1 explains some of the parameters in the model. The  $m$  and  $f$  signify leader or follower, while the  $L$  denotes that the value is the length of a body part. The final letter in each of the variables denotes a specific segment of the body. These parameters were used extensively in the calculations for moment of inertia, location of the center of mass, and value of the torques involved in the spin.

### 2.2 Defining Angles

The angles between various joints and the horizon were the only decision variables in our optimization problem. The joint angles define the dancer’s pose. Table 2.2 explains the label for each angle and gives starting values for the optimization process.

Also, note in Table 2.2 the labeling “push” and “grind”. These words were used to distinguish between the two legs. When we originally discussed the problem with two feet and viewed videos of dancers we determined that one of the feet stayed closer

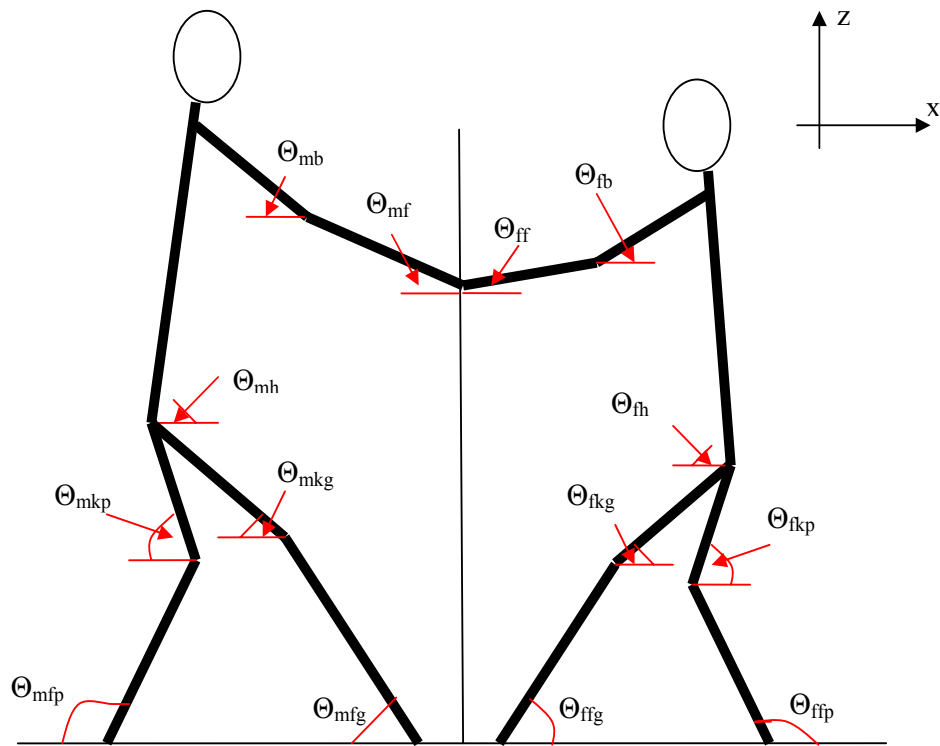


Figure 1: Each dancer's pose is defined by seven joint angles as shown.

Angles			
$\theta_{mf}$	Angle of Forearms	$-\pi/4$	$\pi/2$
$\theta_{mb}$	Angle of Biceps	0	$\pi/2$
$\theta_{mh}$	Angle of Hip	$\pi/4$	$3\pi/4$
$\theta_{mkg}$	Angle of Knee Grind	0	$\theta_{mfg}$
$\theta_{mkp}$	Angle of Knee Push	0	$\theta_{mfp}$
$\theta_{mfg}$	Angle of Foot Grind	0	$\pi$
$\theta_{mfp}$	Angle of Foot Push	0	$\pi$
$\theta_{ff}$	Angle of Forearms	$-\pi/4$	$\pi/2$
$\theta_{fb}$	Angle of Biceps	0	$\pi/2$
$\theta_{fh}$	Angle of Hip	$\pi/4$	$3\pi/4$
$\theta_{fkg}$	Angle of Knee Grind	0	$\theta_{ffg}$
$\theta_{fkp}$	Angle of Knee Push	0	$\theta_{ffp}$
$\theta_{ffg}$	Angle of Foot Grind	0	$\pi$
$\theta_{ffp}$	Angle of Foot Push	0	$\pi$

Table 2: Angle notation with upper and lower bounds

to the axis of rotation and was mainly used for balance. The closer "grind" foot did not contribute to the spin, but countered it by grinding on the floor. The other leg was further from the axis of rotation and was used to "push" the dancer around the circle and thus we labeled the left foot the push foot and the right foot the grind foot.

### 2.3 Calculating Distances to Axis of Rotation

We used trigonometry to calculate the distance from each point on the body to the axis of rotation based on the pose and the parameters for each couple. The hands were assumed to be at the axis of rotation, defined as zero. From that point the rest of the body was defined. A full description of the variables used to represent the distance to the axis of rotation for each joint in the body follows in the next Section.

Each distance from the axis of rotation, the z-axis, to the locations of the body's joints was labeled  $R$  and had a subscript denoting a part of the body. The body parts were labeled subscript  $e$  for elbow,  $s$  for shoulder,  $h$  for hip,  $kg$  and  $kp$  for knee grind and knee push, and finally  $fg$  and  $fp$  for foot grind and foot push. The lengths of each piece,  $L$ , and angles to the horizon,  $\theta$ , were similarly labeled with subscripts. For example, the distance from the elbow to the axis of rotation was defined as  $R_e = L_f * \text{Cos}[\theta_f]$ . The distance to the shoulder is based on the length of the upper arm and the distance to the elbow,  $R_s = L_b * \text{Cos}[\theta_b] + R_e$ . All other distances are calculated based on the distances to the body joints calculated before it.

Body Mass Notation	
$mmt$	mass of leader's torso
$mmq$	mass of leader's quad
$mmc$	mass of leader's calf
$mmb$	mass of leader's bicep
$mmf$	mass of leader's forearm
$fmt$	mass of follower's torso
$fmq$	mass of follower's quad
$fmc$	mass of follower's calf
$fmb$	mass of follower's bicep
$fmf$	mass of follower's forearm

Table 3: Notation for the estimated mass of each body part based on the dancers overall mass.

Therefore the distances between each of the feet and the axis of rotation is determined by the length parameters of the person and the angles of his pose.

## 2.4 Defining Body Segment Masses

To fully define the bodies, we also considered the mass of each body part. In order to estimate this mass we used a system developed by Nickolova to divide the total mass of the body into fractions of the total mass that existed in each body part [3]. Each dancer's total mass was self-reported by the dancers. Table 3 provides the notation used for the mass of each body part.

## 3 Constraining the Model

In addition to defining the size parameters of each dancer and defining his pose, our model also had to consider the ways a person could actually move. For example, in an unconstrained model, each joint angle could take any value. If unconstrained, the joint representing the knee could be bent completely backwards, or the dancer might be in a limbo position where their back is parallel to the ground and their hips are thrust inward.

We added a restriction on the hips, so the hips could not thrust inward. Even though people can thrust their hips inward somewhat, we know from observing dancers that it is not a pose from which one can easily start spinning. The hip

constraints are represented by the following inequalities:

$$\begin{aligned}\theta_{mh} + \theta_{mkg} &\leq \pi \\ \theta_{mh} + \theta_{mkp} &\leq \pi \\ \theta_{fh} + \theta_{fkg} &\leq \pi \\ \theta_{fh} + \theta_{fkp} &\leq \pi\end{aligned}$$

Also, human knees have a limited range of motion. They cannot be bent backwards. As they are defined in our model, the angle at the feet ( $\theta_{ffg}, \theta_{mfg}$ ) must always be greater than ( $\theta_{fkg}, \theta_{mkg}$ ) the angle of the knee. These constraints are represented by:

$$\begin{aligned}\theta_{mkp} - \theta_{mfp} &\leq 0 \\ \theta_{mkg} - \theta_{mfg} &\leq 0 \\ \theta_{fkp} - \theta_{ffp} &\leq 0 \\ \theta_{fkg} - \theta_{ffg} &\leq 0\end{aligned}$$

The elbow also has a limited range of motion. We are limiting the movement of the shoulder to the 2-dimensional yz-plane. Any pose with the elbow bent backward would require the elbow to be broken. The elbow constraints are represented:

$$\begin{aligned}\theta_{mb} - \theta_{mf} &\geq 0 \\ \theta_{fb} - \theta_{ff} &\geq 0\end{aligned}$$

The final constraint that is strictly a function of pose is a constraint on the value of the hip angle. Early in our optimization attempts we would occasionally get a value for the angle of the hip that was negative or near zero. Any angle at or below zero creates a pose where the dancer is entirely bent forward with her torso nearly level with the floor. While this pose creates a small moment of inertia, it is biomechanically unreasonable. The hip constraint is simply:

$$\begin{aligned}\theta_{mh} &\geq \frac{\pi}{4} \\ \theta_{fh} &\geq \frac{\pi}{4}\end{aligned}$$

All of the above constraints ensure that the only allowable pose outputs from the optimization are biologically reasonable poses. We did not want to overly constrain our solution. The constraints listed above should only require that the dancer be in a pose that a human being could assume and spin in.

In addition to the constraints required to make the pose humanly attainable, we also add restrictions on the ranges of the feet and each of the joints to the axis



of rotation. An optimization scheme could determine the best pose would place a dancer's feet on the other side of the axis of rotation crossed over his partner's feet. This pose is a difficult position from which to begin rotating and not particularly stable (dancers might trip).

To eliminate this pose and any other poses where the dancers might be so close that their lower body ends up invading their partner's body space, we require that the distances to each dancer's joints defined in the model are positive. For example the distance to the leaders grind foot is defined as  $mRfg$ . The  $m$  notes that it is the leader, while the  $fg$  indicates that it is the distance to the grind foot. The  $R$  notes that the variable is distance. The constraints on distances are listed:

$$\begin{aligned}
 mRfg &\geq 0 & fRfg &\geq 0 \\
 mRfp &\geq 0 & fRfp &\geq 0 \\
 mRkg &\geq 0 & fRkg &\geq 0 \\
 mRkp &\geq 0 & fRkp &\geq 0 \\
 mRh &\geq 0 & fRh &\geq 0 \\
 mRs &\geq 0 & fRs &\geq 0 \\
 mRE &\geq 0 & fRE &\geq 0
 \end{aligned}$$

The dancers were connected at the hands. Each of the partners could assume a different pose. The height of each dancer's hands depends on his or her pose. Therefore, we wrote a constraint requiring that the height of the dancers' hands be equal so that they could hold hands:

$$fHhand - mHhand = 0$$

The height of the hip was determined by the pose of the grind leg. However, the height of the hip is separately determined by the pose of the push leg. These two values must be equal, thus they are constrained by the equation:

$$fHh - fHhip = 0$$

The  $fHh$  variable represents the location of the hip as defined by the grind foot and  $fHhip$  represents the height of the hip as defined from the push foot. This constraint prevents the model from creating a disconnected dancer.

As our model is defined, the dancers are pulling on their partner's hands creating a tension between them. We did not consider the potential that the dancers would pose in such a way that they would be pushing on one another. Thus, in order to maintain their balance and not push on their partner the dancers grind feet must be

in front of their respective center of mass:

$$\begin{aligned} fxCoM - fRfg &\geq 0 \\ -mxCoM - mRfg &\geq 0 \end{aligned}$$

This constraint will not allow the optimizer to consider any pose that would require the dancers to be leaning into one another.

## 4 Calculating and Maximizing Angular Acceleration

In modeling the spinning motion of dancers, we use their size parameters to determine the best pose for a couple by maximizing their angular acceleration. This model appears to output realistic poses for the Lindy Hop rhythm circle. The ideal pose is deemed to be a pose that maximizes the angular acceleration of the dancers. The angular acceleration,  $\alpha[\Theta]$ , is calculated as:

$$\alpha[\Theta] = \frac{\tau[\Theta]}{I[\Theta]}$$

$$\Theta = [\theta_{ff}, \theta_{fb}, \theta_{fh}, \theta_{fkg}, \theta_{fkp}, \theta_{ffg}, \theta_{ffp}, \theta_{mf}, \theta_{mb}, \theta_{mh}, \theta_{mkg}, \theta_{mkp}, \theta_{mfg}, \theta_{mfp}]$$

where  $\tau[\Theta]$ , is the scalar torque produced by the dancer in the direction perpendicular to the floor as a function of  $\Theta$ . The moment of inertia,  $I[\Theta]$ , is the dancers' resistance to initiating a spin. Theta,  $\Theta$ , is a vector of angles that define both dancers' poses.

The first step in determining  $\alpha[\Theta]$  is to determine the moment of inertia. To calculate the moment of inertia we treated the body segments as non-right cylinders and used integrals along with the formula for the moment of inertia of a disk rotating around an axis.

### 4.1 Parallel Axis Theorem

We calculated the moment of inertia of each body segment in a given pose by twice applying the parallel axis theorem. The parallel axis theorem allows us to find the moment of inertia of a body rotating around an axis by providing a mechanism for calculating the moment of inertia around the center of mass of that body and then shifting the object over a specified amount. The parallel axis theorem states:

$$I_{new} = I_{com} + Md^2$$

where  $I_{new}$  is the moment of inertia of the body rotating around an axis at some distance,  $d$ , from its center of mass,  $I_{com}$  is the moment of inertia of the object around its center of mass, and  $M$  is the mass of the object.

In our model, the dancer's body was defined as a collection of possibly non-right cylinders. To find the moment of inertia of the dancer, we find the moment of inertia of each part of the body and then sum the individual moments of inertia. To find the moment of inertia of a single body part modeled as a non-right cylinder we applied the parallel axis theorem as an integral over the length of the cylinder.

## 4.2 Integrals over non-right cylinders

Integrals were used because integrals can represent a sum of infinitely thin objects stacked on top of one another. Using the moment of inertia of a thin disk,  $I_{disk} = \frac{1}{2} * M * R_{disk}^2$ , and then taking the integral over the length of the non-right cylinder to sum the moments of inertia of the individual disks, we can calculate the moment of inertia of the cylinder rotating around its center of mass.

Figure 2 shows an example of a non-right cylinder and labels how all of the variables in the integration would be labeled. The radius of the cylinder is labeled  $r_{cylinder}$  and is also the radius of the thin disk. The distance that each disk would be offset from the center of mass of the cylinder is labeled  $r$  and  $R$  is the distance from the center of mass of the cylinder to the axis the dancer is rotating around. The calculations for the moment of inertia of a single body part are illustrated below. We begin by calculating the moment of inertia of a single thin disk:

$$I_{disk} = \frac{1}{2}R_{cylinder}^2 + Mr^2$$

Integrating over the length of the cylinder sums the moments of inertia of the individual disks and determines the moment of inertia of the whole cylinder. We also use the parallel axis theorem again by adding an additional  $MR^2$  term that will account for the shift of the cylinder from rotating around its own center of mass to rotating around a center of mass some distance away. The new inertia would be represented as:

$$I_{segment} = \int_{r_o}^{r_1} I_{disk}dr + MR^2$$

Combining the two equations listed above, we calculate the moment of inertia of the body segment rotating around the axis of rotation of the dancer's spin as:

$$I_{segment} = \int_{r_o}^{r_1} (\frac{1}{2}R_{cylinder}^2 + Mr^2)dr + MR^2$$

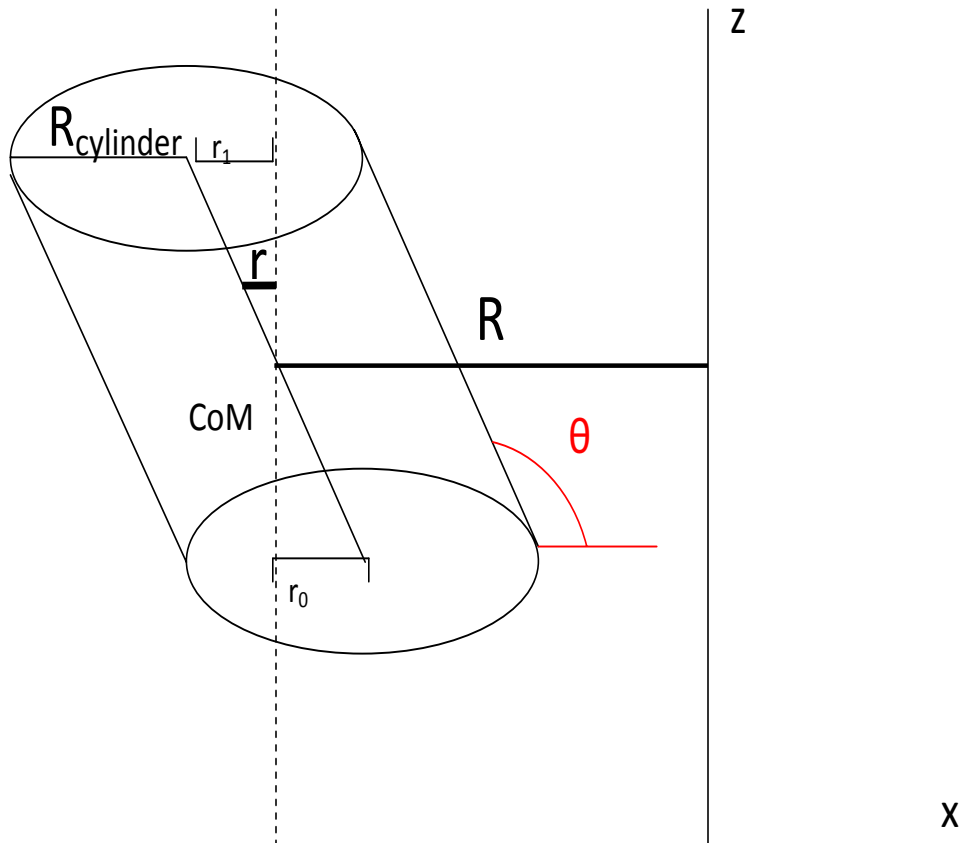


Figure 2: A model of the cylinder that defines the different variables used in the integration for the moment of inertia.

As an example of the above calculation we can look at the results for one of the body parts. The above calculations result in an equation for the moment of inertia of the torso of:

$$\begin{aligned}
 fInertiaTorso = & \\
 & \frac{1}{2}fmt * frt^2 + \\
 & \frac{1}{12}fLt^2 * fmt * Cos[\theta_{fh}]^2 * Sin[\theta_{fh}] + \\
 & fmt * (fRs + \frac{1}{2}fRh)^2
 \end{aligned}$$

where  $\frac{1}{2}fmt * frt^2$  is the inertia for a single thin disk around its center of mass. The  $\frac{1}{12}fLt^2 * fmt * Cos[\theta_{fh}]^2 * Sin[\theta_{fh}]$  is the result of the integral that sums all of the disks over the length of the cylinder. Finally the  $fmt * (fRs + \frac{1}{2}fRh)^2$  term equates to the  $MR^2$  term above and shifts the entire moment of inertia from rotating around its own center to rotating around the axis some distance away. The length and angle variables are defined in Tables 1 and 2.2.

### 4.3 Calculating Torque

Calculating the correct,  $\tau[\Theta]$ , was the most challenging parts of building the model. Torque,  $\tau$ , the rotational analog of force causes an object to spin and produces angular acceleration. While torque is in fact a vector with magnitude and direction, we only considered the torque relating to the dancers' partnered spin around each other on the floor and thus treated it as a scalar. Tau can not be arbitrarily large because the force is generated by the dancer pushing against the floor, and there is a limit beyond which the dancer's foot will slip. All of the external forces acting on the dancers are related to one another. Figure 3 illustrates all of these forces acting on the dancers. There are in fact only four independent forces at work as the dancer spins: the force of gravity acting through the center of mass, the force acting at her hands from her partner pulling on her, and the force from the floor acting on each of her two feet.

In Figure 3 each of these forces is separated into components in the x,y, and z axes. We set the force acting at the hands in the y and z axes to be zero. Thus the force at the hands is only represented by a single arrow in this picture. The forces on each of the feet were separated into their x,y,z components.

The known force of gravity acts through the center of mass of the dancer in the z-direction and is equal to 9.8 meters per second squared times  $fMass$ . The force in the x-direction on the follower from her partner pulling on her hands is  $fFxHands$ , while  $mFxHands$  is the equivalent force on the leader from the follower pulling on his hands. While  $fFyHands$ ,  $fFzHands$ ,  $mFyHands$ , and  $mFzHands$  do exist,

they are not illustrated because for the purposes of our model we set them equal to zero.  $fFgrindVert$  is the force in the x-direction on the follower's grind foot that is a result of friction and represents her tendency to slide toward or away from her partner.  $mFgrindVert$  represents the equivalent force to  $fFgrindVert$  for the leader.  $fFpushVert$  is the force in the x-direction on the follower's push foot.  $mFpushVert$  represents the force in the x-direction acting on the leader's push foot.  $fFgrindHort$  and  $fFpushHort$  are the forces acting on each of the follower's feet in the z-direction. These forces are often referred to as normal forces.  $mFgrindHort$  and  $mFpushHort$  are the normal forces on the leader's feet.

Finally  $fFpushSpin$  is the force on the follower's push foot in the y-direction that will induce motion that will initiate the spin. These forces are the most crucial forces in our model because they are the forces that induce the spin. Our goal was to find a method for estimating these forces. This force is countered by  $fFgrindspin$  which is the force in the y-direction at the grind foot.

While there are only 8 external forces controlling this system, estimating these forces from the dancers' pose is a challenging problem. One of the first steps in solving it is to determine the location of the center of mass for a dancer in a given pose [5].

Gravity acts through an object's center of mass. We used our segmented body model to calculate the center of mass, and we calculated the x, y, and z components of the center of mass separately. The center of mass of each body segment is the average of the two end points of a body part.

For example, the x-coordinate of the center of the torso is  $xCoMt = (Rs + Rh)/2$ , where  $Rs$  and  $Rh$  are the distances from the axis of rotation to the shoulder and the hip, respectively. These distances were calculated using trigonometry. A weighted average of these values determined x-coordinates of the center of mass of the body. Similar calculations yield the location of the z-coordinate of the center of mass using heights instead of distances to the axis of rotation. Because our model did not allow for any movement in the y-axis, we set the y-coordinate of the center of mass to zero.

To determine the weight of each body part we used work by Nikolova and Toshev on the population of Bulgaria [3]. They developed a standard for the percentage of a person's weight that is in each of his or her body parts. While this method will not provide a precise distribution for each individual, it allows us to easily estimate the distribution for all of the subjects.

To find the six unknown forces we defined earlier, we considered them as a part of the whole system that defined the movements of the dancers. Our full model had 27 degrees of freedom. Unfortunately when we attempted to solve this model we were unable to obtain a solution to the equations even though we attempted several different methods for solving the system. In the end we used a surrogate method for estimating the forces applied by the dancers.

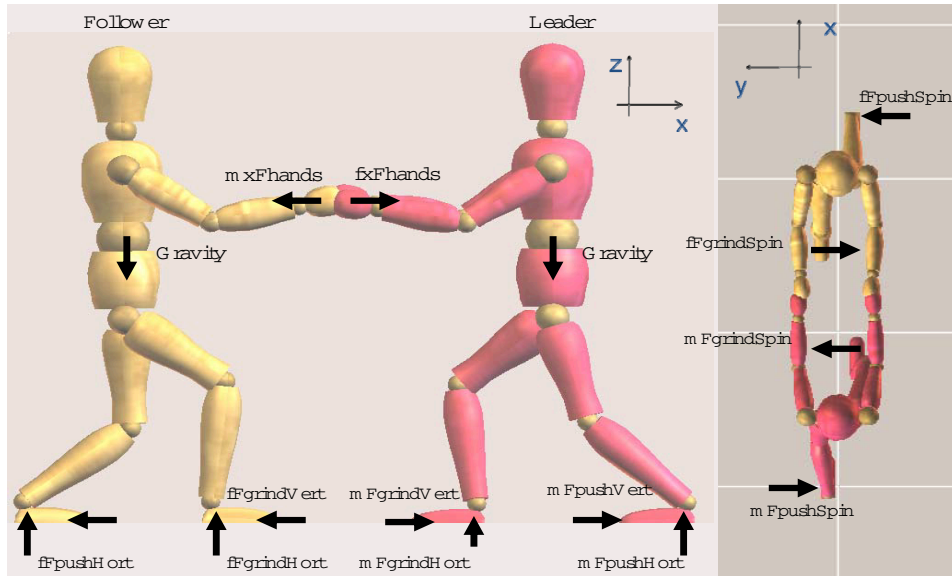


Figure 3: All of the forces acting on the system to cause it to rotate.

## 5 Developed Mathematical Model

Ultimately to model the dancers we used a simpler model that neglected  $F_{hands}$ , forces on the grind foot, and used a surrogate,  $NormalPush$  for  $F_{pushSpin}$ . We assume that the reaction forces from the floor are equal to the weight of the person over their push foot, which we estimate using the location of their center of mass. The feet are separated in the  $y$ -direction. We calculate the distance from the axis of rotation to the feet using Pythagorean theorem. The calculations for these distances for the follower ( $f$ ) and the leader ( $m$ ) were:

$$fDistPush = \sqrt{(fxCoM - fRfp)^2 + frt^2} \quad (1)$$

$$fDistGrind = \sqrt{(fxCoM - fRfg)^2 + frt^2} \quad (2)$$

$$mDistPush = \sqrt{(mxCoM - mRfp)^2 + mrt^2} \quad (3)$$

$$mDistGrind = \sqrt{(mxCoM - mRfg)^2 + mrt^2} \quad (4)$$

The variables used above represent the location of the center of mass minus the distance to the axis of rotation, plus the radius of the body segment, which takes into account the physical size of the body segment. Using these distances we estimated what fraction of their weight was supported by their push foot:

$$fWeightPush = \frac{fDistGrind}{fDistGrind + fDistPush} \quad (5)$$

$$mWeightPush = \frac{mDistGrind}{mDistGrind + mDistPush} \quad (6)$$

If the dancer is standing mostly over her push foot, then the distance between her center of mass and grind foot will be large. By the equation above, this larger distance will equate to a larger fraction of her weight being over her push foot. Conversely, if  $fDistGrind$  is small than most of the dancer's weight is over her grind foot not her push foot thus a small value for  $fDistGrind$  corresponds to a smaller value for  $fWeightPush$ . By taking the product of the fraction of their weight over their push foot and their weight, we determined the normal force acting on the dancer's foot:

$$fNormalPush = fWeightPush * fMass * gravity \quad (7)$$

$$mNormalPush = mWeightPush * mMass * gravity \quad (8)$$

Using these normal forces, the simplifying assumption that the dancer would not push with any force in the x-direction and a an estimation of  $\mu s$ , the coefficient of static friction, we made the claim that the normal force on the push foot is proportional to  $fFpushSpin$ . With this assumption we can calculate the push force to be:

$$fForcePush = fRfp * fNormalPush * \mu s \quad (9)$$

$$mForcePush = mRfp * mNormalPush * \mu s \quad (10)$$

Since both the leader and follower contribute to the force that causes the couple to spin, we sum these forces and divide by  $InertiaTotal$  to estimate the angular acceleration:

$$\alpha = \frac{fForcePush + mForcePush}{InertiaTotal} \quad (11)$$

Even in this simple form, the model still contained 14 degrees of freedom. This simple model performed surprisingly well, giving us reasonable outputs for  $\alpha$  in both the actual pose and the optimal pose, as well as plausible optimal poses. Figure 4 for an illustration of the model explained and refer to Section 7 for images of the actual and optimal poses, and values for  $\alpha$ .

## 6 Numerical Optimization

One challenging aspect of this project is optimizing the function estimating the angular acceleration of the dancers. We used the "NMaximize" function in Mathematica as our numerical optimization algorithm. Originally we planned to analytically determine a constrained function to represent the optimal pose. We discovered that our



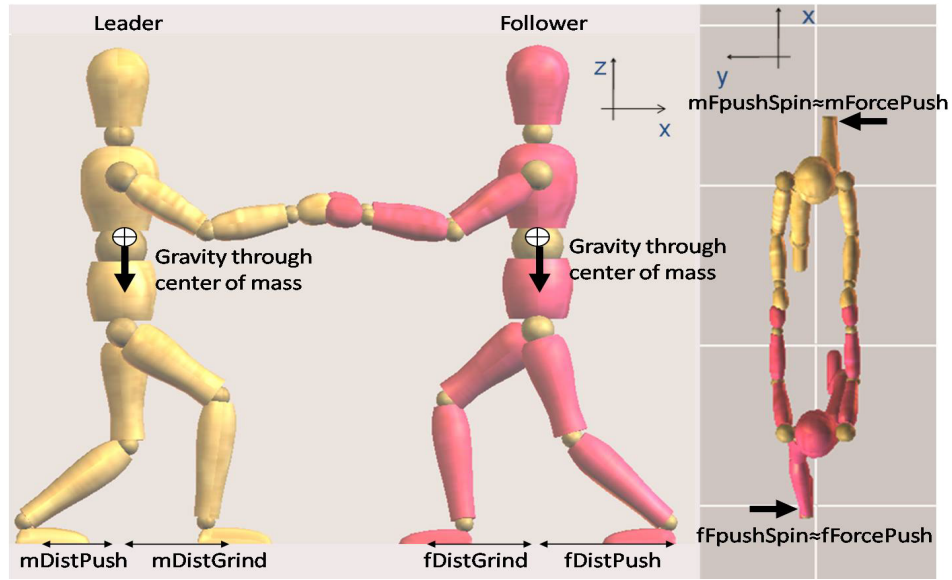


Figure 4: This figure illustrates the calculations for the surrogate model.

system was too complicated to determine an analytic solution. For each couple, we used individual size length and mass parameters to determine that couple's optimal and achieved accelerations, solving a unique optimization problem for each couple.

We maximized  $\alpha$ , the rotational acceleration estimate for the couple, subject to biological feasibility constraints on the pose, using Mathematica's NMaximize function. For a list of constraints see Section 3. The decision variables are the fourteen pose angles.

One limitation of NMaximize is its sensitivity to the starting pose used for the optimization. The starting pose is specified as a range of values for each decision variable, from which the algorithm starts its search. The optimizer may get stuck in a local optimum near the starting solution. We started each search around the pose the couple actually held. While the optimal pose is very different from the initial pose, we discovered that the value of the objective at optimal varied even with slight changes in the initial pose.

We sought the global maximum for the angular acceleration. The global maximum is the highest angular acceleration of any pose that fits the constraints and parameters of the problem. Finding the global optimum is much more difficult than finding a local optimum, which would just be the nearest peak or valley in the solution. Methods for global optimization generally use a combination of random start points and local optimization techniques to find the global optimum. At times Mathematica did not reach a global optimum, but instead got stuck in a local optimum. The variation in

Achieved and Optimal Angular Acceleration				
Couple	Class	Achieved	Optimal	Fraction of Optimal
A	Expert	4.50093	45.9221	0.0980
B	Beginner	3.22323	44.6527	0.0722
C	Expert	6.44338	48.0171	0.1368
D	Beginner	3.49177	48.6595	0.0718
E	Expert	3.49527	49.8348	0.0701
F	Expert	4.972	47.3274	0.1056
G	Beginner	3.96729	49.8875	0.0795
I	Beginner	3.95054	45.0883	0.0876
J	Beginner	4.28396	42.431	0.1010

Table 4: Achievable and optimal acceleration for each couple and the fraction of optimal angular acceleration they achieved.

the “optimal” solution, as described in the previous paragraph, is evidence of failure to consistently find the true global optimum.

## 7 Data Analysis and Results

Our mathematical model predicts the achievable rotational acceleration for each pair of dancers in any fixed pose. Using numerical optimization we determined the best pose and corresponding highest rotational acceleration. The measurements of the pose the dancers actually used in their partnered spin are input into the same model to compute the achievable acceleration in that pose. We calculated a ratio of each couple’s achievable acceleration in the observed pose to that of the optimal pose. A larger ratio means that the pair is achieving a higher fraction of their potential acceleration. Table 4 lists the achieved and optimal angular accelerations for each couple along with the fraction of optimal.

Couple H is not listed in the table because we were not able to garner reasonable data from the couple. Because of the pose in which they were standing and the limitations our model put on the rotation of the hip joint, Couple H’s actual pose was infeasible by the definitions of our model. We did not observe this issue with any of the other couples recorded.

Since each dancer has different size parameters, the optimal poses and maximum achievable accelerations differ between the couples. We compared each couple’s performance to their individual optimum. We hypothesized that the best couples would achieve a higher fraction of their optimum than less skilled dancers.

---

With our motion capture system, we could record an observed rotational acceleration. However, we still calculated an estimate of acceleration based on our simplified model, because we determined a fraction of optimal performance based on the optimal acceleration from the same model. Using the achievable acceleration in the actual poses calculated from the same model provided a metric for comparing the couples' performances.

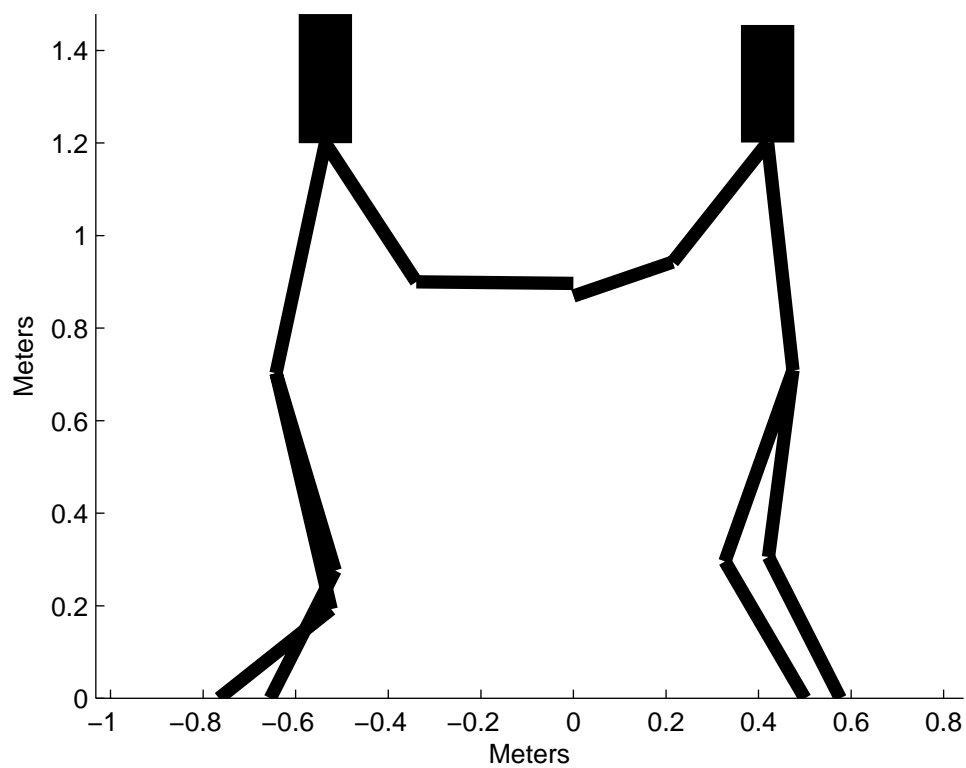
To test our hypothesis, we used the Mann-Whitney statistical test to compare these numbers across couples. We first divided the couples into two categories, beginners and experts. The couples' fractions of optimal are then ranked from largest to smallest. With their ranks the fractions are then separated back into their categories and the ranks are summed together. This test is a one-tailed test, where we expect to find that if there is any difference between the categories, the experts will have a larger fraction of optimal. Using a table from Rice's statistics book [4], we determined whether the two categories we ranked differed. We did not find a difference between the two categories at an  $\alpha = .05$  level of statistical significance.

Our small dataset may have contributed to our inability to find a significant difference between expert and beginner couples. We captured twenty different couples, but we were only able to process data from 10 of the couples. While we cannot reach any firm conclusions, we can draw some interesting anecdotal observations based on the optimal poses that our model calculated.

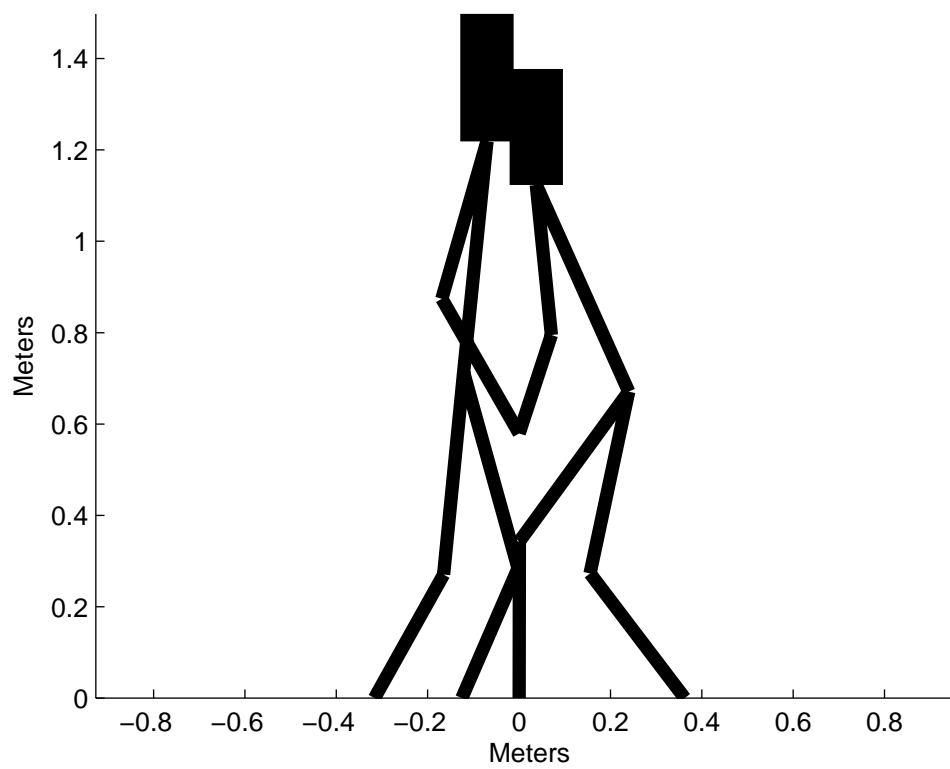
All of our couples' optimal poses are very similar and seem intuitively logical. To spin fast the couples need to get close together and put their feet in close to the center of the circle. The push foot does need to have some distance to the axis of rotation so it can produce the torque required to initiate the spin. See Figure 5 for an example of an optimal and actual pose.

## 7.1 Model Shortcomings

In this project, we necessarily neglected a number of elements related to a partnered spin: the ease or difficulty with which people are able to hold various poses (internal forces), the need to see your partner, the more complicated arm connection points, the freedom of many joints like the shoulder and hip to move in more than a hinge fashion, the push versus grind phase of the spin, and the possibility that the dancers might be considering anesthetics instead of physics in their selection of a pose. Perhaps these simplifications explain why we saw none of the couples adopt a pose that is close to the optimal pose predicted by our model.



(a) The actual pose the dancers held



(b) The optimal pose as calculated by the model

Figure 5: The actual and optimal poses for couple A.



Figure 6: The pose dancers assume to spin. One arm is around their partners' shoulder (closed arm) and one grasping their partners' hand (open hand).

### 7.1.1 Hand Simplification

In retrospect, the decision to combine the various points of connection between the leader and follower into one link located at the leader's left and follower's right hand may have been pivotal. Recording the neglected closed arm connection, between the leader's right arm and the follower's back, would have made our "actual" poses seem much closer together than they appeared in our calculations. The closed arm around the back connection is generally considered a stronger and more useful connection in this type of spin and indeed in this dance than the connection at the open hands. By describing the dancers' actual performance in terms of the distance between their open hand-to-hand connection, we may have chosen a very noisy observation of the true distance between their torsos. Figure 6 illustrates the pose dancers spin in and shows how much closer the dancers are on their closed shoulder side. These dancers have a large distance between their open hands, which was the distance we considered for our model.

### 7.1.2 Dimensional Simplification

Our model is superficially a 3D model but is essentially planar. In the future work should begin from a more complex three-dimensional model. While this might add more variables to an already complex problem, a more detailed model would allow for the full consideration of the closed position with a hand creating force at the shoulder

and the other hand connecting to his partner. Additionally, a more biologically detailed three-dimensional model would allow “lean” in the pose, so a dancer might shift his or her weight in the y-direction to gain more torque.

When reviewing video and pictures of dancers we noticed that in some cases the dancers do not exactly face one another. The dancers’ shoulders on the closed side, with the arm around the back connection, are much closer together than their shoulders on the open hand-to-hand connection side. Our model could not account for this twist. We could have partially addressed this limitation by examining the distance between the shoulders and making that the distance between the dancers. This technique would eliminate the consideration of the open hand.

## 8 Conclusion

### 8.1 Project Summary

In undertaking this work we hoped to understand the pose a swing dancer selects to complete a rhythm circle. We built a mathematical model to predict the optimal pose for a dance couple based on the leader’s and follower’s specific size parameters. With this model we estimated the external forces on the system and the moment of inertia of the couple. We calculated the angular acceleration of the couple and placed biologically reasonable constraints on the poses. Using numerical optimization we computed the “best” pose and compared it to the pose the couple actually held as shown from our motion capture system.

Analyzing our results, we find that the optimal pose predicted is logical. Qualitatively the optimum poses that we found are in very good agreement with what expert dancers would teach students about this partnered spin. Dance teachers usually advise that this spin works better the closer one can get to one’s partner and that the right (grind) foot should be at or close to the axis of rotation while the left (push) foot should be farther away. Additionally, we were looking to determine if there was a difference between the fraction of optimal achieved by beginners and expert dancers. No statistically significant difference at the  $\alpha = .05$  level was found. The angular acceleration achieved by the couples was a factor of ten less than the predicted optimal acceleration. No couples in fact came close to their optimal acceleration. We examined a number of areas that might have been the cause of this large difference between achieved and optimal acceleration.

## 8.2 Accomplishments

One of the major accomplishments of this project is bringing a useful motion capture system to the Naval Academy. Prior to this project, no equipment or program for advanced motion capture study existed. The system setup we used for this project can track up to 24 points and handle very complex motions. Also, as a result of this project we have an archive of data of swing dancers, which later students could re-use.

We built a completely new model of a dance couple. Our model was not based on a previously developed model, but was literally built from the ground up. We defined the joint angles to draw an understanding of the pose the dancers were in and used the lengths of the actual couples' bodies to define the lengths of the model. To determine the optimal pose, we developed a method for estimating the forces at the feet and used an algorithm for maximizing the angular acceleration.

As a result of this model and the data collected we were able to perform a statistical significance test on ten couples to compare the fraction of optimal acceleration obtained by expert and beginning dancers. We also obtained images of the optimal poses that might be useful in helping dancers and dance teachers to better understand the optimal technique for spinning fast.

## Acknowledgments

I would like to thank my advisors for this work Assistant Professor Sommer E. Gentry of the USNA Math Department and Associate Professor Kevin L. McIlhany of the Physics Department for their guidance, assistance and advice through out my work on this project.

## References

- [1] Kenneth Laws. Momentum transfer in dance. *Medical Problems of Performing Artists*, 13(136–145), 1998.
- [2] Kenneth Laws. *Physics and the art of dance Understanding movement*. Oxford University Press, Mar 2005.
- [3] Gergana Stefanova Nikolova and Yuli Emilov Toshev. Estimation of male and female body segment parameters of the bulgarian population using a 16-segmental mathematical model. *Journal of Biomechanics*, 40:3700–3707, 2007.
- [4] John Rice. *Mathematical Statistics and Data Analysis*. Duxbury Press, 1995.

- [5] Aydin Tozeren. *Human Body Dynamics: Classical Mechanics and Human Movement*. Springer, 2000.